RECOMMENDATION ITU-R P.618-6

PROPAGATION DATA AND PREDICTION METHODS REQUIRED FOR THE DESIGN OF EARTH-SPACE TELECOMMUNICATION SYSTEMS

(Question ITU-R 206/3)

(1986-1990-1992-1994-1995-1997-1999)

The ITU Radiocommunication Assembly,

considering

a) that for the proper planning of Earth-space systems it is necessary to have appropriate propagation data and prediction techniques;

b) that methods have been developed that allow the prediction of the most important propagation parameters needed in planning Earth-space systems;

c) that as far as possible, these methods have been tested against available data and have been shown to yield an accuracy that is both compatible with the natural variability of propagation phenomena and adequate for most present applications in system planning,

recommends

1 that the methods for predicting the propagation parameters set out in Annex 1 be adopted for planning Earth-space radiocommunication systems, in the respective ranges of validity indicated in the Annex.

NOTE 1 – Supplementary information related to the planning of broadcasting-satellite systems as well as maritime, land, and aeronautical mobile-satellite systems, may be found in Recommendations ITU-R P.679, ITU-R P.680, ITU-R P.681 and ITU-R P.682, respectively.

ANNEX 1

1 Introduction

In the design of Earth-space links for communication systems, several effects must be considered. Effects of the non-ionized atmosphere need to be considered at all frequencies, but become critical above about 1 GHz and for low elevation angles. These effects include:

a) absorption in atmospheric gases; absorption, scattering and depolarization by hydrometeors (water and ice droplets in precipitation, clouds, etc.); and emission noise from absorbing media; all of which are especially important at frequencies above about 10 GHz;

b) loss of signal due to beam-divergence of the earth-station antenna, due to the normal refraction in the atmosphere;

c) a decrease in effective antenna gain, due to phase decorrelation across the antenna aperture, caused by irregularities in the refractive-index structure;

d) relatively slow fading due to beam-bending caused by large-scale changes in refractive index; more rapid fading (scintillation) and variations in angle of arrival, due to small-scale variations in refractive index;

e) possible limitations in bandwidth due to multiple scattering or multipath effects, especially in high-capacity digital systems;

f) attenuation by the local environment of the ground terminal (buildings, trees, etc.);

g) short-term variations of the ratio of attenuations at the up- and down-link frequencies, which may affect the accuracy of adaptive fade countermeasures;

h) for non-geostationary satellite (non-GSO) systems, the effect of varying elevation angle to the satellite.

Ionospheric effects (see Recommendation ITU-R P.531) may be important, particularly at frequencies below 1 GHz. For convenience these have been quantified for frequencies of 0.1; 0.25; 0.5; 1; 3 and 10 GHz in Table 1 for a high value of total electron content (TEC). The effects include:

j) Faraday rotation: a linearly polarized wave propagating through the ionosphere undergoes a progressive rotation of the plane of polarization;

k) dispersion, which results in a differential time delay across the bandwidth of the transmitted signal;

l) excess time delay;

m) ionospheric scintillation: inhomogeneities of electron density in the ionosphere cause refractive focusing or defocusing of radio waves and lead to amplitude fluctuations termed scintillations. Ionospheric scintillation is maximum near the geomagnetic equator and smallest in the mid-latitude regions. The auroral zones are also regions of large scintillation. Strong scintillation is Rayleigh distributed in amplitude; weaker scintillation is nearly log-normal. These fluctuations decrease with increasing frequency and depend upon path geometry, location, season, solar activity and local time. Table 2 tabulates fade depth data for VHF and UHF in mid-latitudes, based on data in Recommendation ITU-R P.531.

   Accompanying the amplitude fluctuation is also a phase fluctuation. The spectral density of the phase fluctuation is proportional to $1/f^3$, where f is the Fourier frequency of the fluctuation. This spectral characteristic is similar to that arising from flicker of frequency in oscillators and can cause significant degradation to the performance of receiver hardware.

This Annex deals only with the effects of the troposphere on the wanted signal in relation to system planning. Interference aspects are treated in separate Recommendations:

– interference between earth stations and terrestrial stations (Recommendation ITU-R P.452);

– interference from and to space stations (Recommendation ITU-R P.619);

– bidirectional coordination of earth stations (Recommendation ITU-R P.1412).

An apparent exception is path depolarization which, although of concern only from the standpoint of interference (e.g. between orthogonally-polarized signal transmissions), is directly related to the propagation impairments of the co-polarized direct signal.

The information is arranged according to the link parameters to be considered in actual system planning, rather than according to the physical phenomena causing the different effects. As far as possible, simple prediction methods covering practical applications are provided, along with indications of their range of validity. These relatively simple methods yield satisfactory results in most practical applications, despite the large variability (from year to year and from location to location) of propagation conditions.

As far as possible, the prediction methods in this Annex have been tested against measured data from the data banks of Radiocommunication Study Group 3 (see Recommendation ITU-R P.311).

2 Propagation loss

The propagation loss on an Earth-space path, relative to the free-space loss, is the sum of different contributions as follows:

– attenuation by atmospheric gases;

– attenuation by rain, other precipitation and clouds;

– focusing and defocusing;

– decrease in antenna gain due to wave-front incoherence;

– scintillation and multipath effects;

– attenuation by sand and dust storms.

TABLE 1

Estimated* ionospheric effects for elevation angles of about 30° one-way traversal**

(derived from Recommendation ITU-R P.531)

Effect	Frequency dependence	0.1 GHz	0.25 GHz	0.5 GHz	1 GHz	3 GHz	10 GHz
Faraday rotation	$1/f^2$	30 rotations	4.8 rotations	1.2 rotations	108°	12°	1.1°
Propagation delay	$1/f^2$	25 µs	4 µs	1 µs	0.25 µs	0.028 µs	0.0025 µs
Refraction	$1/f^2$	< 1°	< 0.16°	< 2.4′	< 0.6′	< 4.2″	< 0.36″
Variation in the direction of arrival (r.m.s.)	$1/f^2$	20′	3.2′	48″	12″	1.32″	0.12″
Absorption (auroral and/or polar cap)	$\approx 1/f^2$	5 dB	0.8 dB	0.2 dB	0.05 dB	6×10^{-3} dB	5×10^{-4} dB
Absorption (mid-latitude)	$1/f^2$	< 1 dB	< 0.16 dB	< 0.04 dB	< 0.01 dB	< 0.001 dB	$< 10^{-4}$ dB
Dispersion	$1/f^3$	0.4 ps/Hz	0.026 ps/Hz	0.0032 ps/Hz	0.0004 ps/Hz	1.5×10^{-5} ps/Hz	4×10^{-7} ps/Hz
Scintillation[(1)]	See Rec. ITU-R P.531	See Rec. ITU-R P.531	See Rec. ITU-R P.531	See Rec. ITU-R P.531	>20 dB peak-to-peak	≈ 10 dB peak-to-peak	≈ 4 dB peak-to-peak

* This estimate is based on a TEC of 10^{18} electrons/m^2, which is a high value of TEC encountered at low latitudes in day-time with high solar activity.

** Ionospheric effects above 10 GHz are negligible.

(1) Values observed near the geomagnetic equator during the early night-time hours (local time) at equinox under conditions of high sunspot number.

TABLE 2

Distribution of mid-latitude fade depths due to ionospheric scintillation (dB)

Percentage of time (%)	Frequency (GHz)			
	0.1	0.2	0.5	1
1.0	5.9	1.5	0.2	0.1
0.5	9.3	2.3	0.4	0.1
0.2	16.6	4.2	0.7	0.2
0.1	25.0	6.2	1.0	0.3

Each of these contributions has its own characteristics as a function of frequency, geographic location and elevation angle. As a rule, at elevation angles above 10°, only gaseous attenuation, rain and cloud attenuation and possibly scintillation will be significant, depending on propagation conditions. For non-GSO systems, the variation in elevation angle should be included in the calculations, as described in § 8.

(In certain climatic zones, snow and ice accumulations on the surfaces of antenna reflectors and feeds can produce prolonged periods with severe attenuation, which might dominate even the annual cumulative distribution of attenuation.)

2.1 Attenuation due to atmospheric gases

Attenuation by atmospheric gases which is entirely caused by absorption depends mainly on frequency, elevation angle, altitude above sea level and water vapour density (absolute humidity). At frequencies below 10 GHz, it may normally be neglected. Its importance increases with frequency above 10 GHz, especially for low elevation angles. This effect is discussed in detail in Recommendation ITU-R P.676.

2.1.1 Procedure for calculating gaseous attenuation

The method described below should be used to calculate the median gaseous absorption loss expected for a given value of surface water vapour density, ρ_w, for frequencies up to 350 GHz (excluding the 57-63 GHz band for which information may be obtained from Recommendation ITU-R P.676).

Parameters required for the method include:

f: frequency (GHz)

θ: path elevation angle (degrees)

h_s: height (km) above mean sea level of the Earth terminal; if unknown, a value of $h_s = 0$ will give somewhat conservative results

ρ_w: water vapour density (g/m^3) at the surface (i.e. at height h_s) for the location of interest.

In general, the mean or median value of ρ_w for a month or year is input to the model. Representative median values can be obtained from Recommendation ITU-R P.836. Data are also available from some national weather services. Since the model assumes an averaged height profile for water vapour density, application of the calculation procedure to periods of less than one month may introduce inaccuracies and is not recommended.

Step 1: Calculate the specific attenuations at the surface for dry air γ_o, and water vapour, γ_w, for the frequency, f, and the water vapour density, ρ_w, as specified in Recommendation ITU-R P.676.

Step 2: Compute the equivalent heights for dry air h_o, and water vapour, h_w, as specified in Recommendation ITU-R P.676.

Step 3: Calculate the total slant path gaseous attenuation, A_g, through the atmosphere.

– For $\theta > 10°$:

$$A_g = \frac{\gamma_o \, h_o \, e^{-h_s / h_o} + \gamma_w \, h_w}{\sin \theta} \qquad \text{dB} \tag{1}$$

– For $\theta \leq 10°$:

$$A_g = \frac{\gamma_o \, h_o \, e^{-h_s / h_o}}{g(h_o)} + \frac{\gamma_w \, h_w}{g(h_w)} \qquad \text{dB} \tag{2}$$

with:

$$g(h) = 0.661 \, x + 0.339 \sqrt{x^2 + 5.5 \, (h / R_e)} \tag{3a}$$

$$x = \sqrt{\sin^2 \theta + 2(h_s / R_e)} \tag{3b}$$

where h is to be replaced by h_o or h_w as appropriate.

In this prediction method, R_e is the effective Earth radius after accounting for refraction (see Recommendation ITU-R P.834). Typically, a value of $R_e = 8\,500$ km is appropriate for $h_s \leq 1$ km. (For $h_s > 1$ km, see Recommendation ITU-R P.676.)

Equations (2) to (3b) are engineering formulae derived from equations (28) to (35c) of Recommendation ITU-R P.676, based on the following approximations:

$$\cos \theta \approx 1; \quad \sin^3 \theta \ll \sin \theta; \quad h_s^2 / R_e^2 \ll 4 \, h_s / R_e$$

Note that $x = \sin \theta$ for $h_s = 0$.

2.1.2 Variability of gaseous attenuation

At a given frequency the oxygen contribution to atmospheric absorption is relatively constant. However, both water vapour density and its vertical profile are quite variable, which makes computation of accurate cumulative statistics of gaseous attenuation difficult. Approximate distributions can be obtained from the method of § 2.1.1, if surface water vapour density statistics and concurrent surface temperature information are used. Typically, the maximum gaseous attenuation occurs during the season of maximum rainfall (see Recommendation ITU-R P.836).

Maps illustrating the seasonal variation of absolute humidity at ground level are provided in Recommendation ITU-R P.836. These can be used in the method to estimate the seasonal variation in clear-air attenuation.

For some systems the variations in atmospheric attenuation exceeded for large percentages of the time (when no rain is present) are important. A study of 11.4 GHz sky noise level variations at several locations in Europe showed that seasonal variations in the monthly median level of total attenuation did not exceed 0.1 dB, and that the total attenuation exceeded for 20% of the worst month was 0.05 to 0.15 dB above the monthly median value, depending on location. These attenuations are thought to be caused mainly by water vapour absorption.

2.2 Attenuation by precipitation and clouds

2.2.1 Prediction of attenuation statistics for an average year

The general method to predict attenuation due to precipitation and clouds along a slant propagation path is presented in § 2.2.1.1.

If reliable long-term statistical attenuation data are available that were measured at an elevation angle and a frequency (or frequencies) different from those for which a prediction is needed, it is often preferable to scale these data to the elevation angle and frequency in question rather than using the general method. The recommended frequency-scaling method is found in § 2.2.1.2.

Site diversity effects may be estimated with the method of § 2.2.4.

2.2.1.1 Calculation of long-term rain attenuation statistics from point rainfall rate

The following procedure provides estimates of the long-term statistics of the slant-path rain attenuation at a given location for frequencies up to 55 GHz. The following parameters are required:

$R_{0.01}$: point rainfall rate for the location for 0.01% of an average year (mm/h)

h_s : height above mean sea level of the earth station (km)

θ : elevation angle (degrees)

φ : latitude of the earth station (degrees)

f : frequency (GHz)

R_e : effective radius of the Earth (8 500 km)

The geometry is illustrated in Fig. 1.

FIGURE 1

Schematic presentation of an Earth-space path giving the parameters to be input into the attenuation prediction process

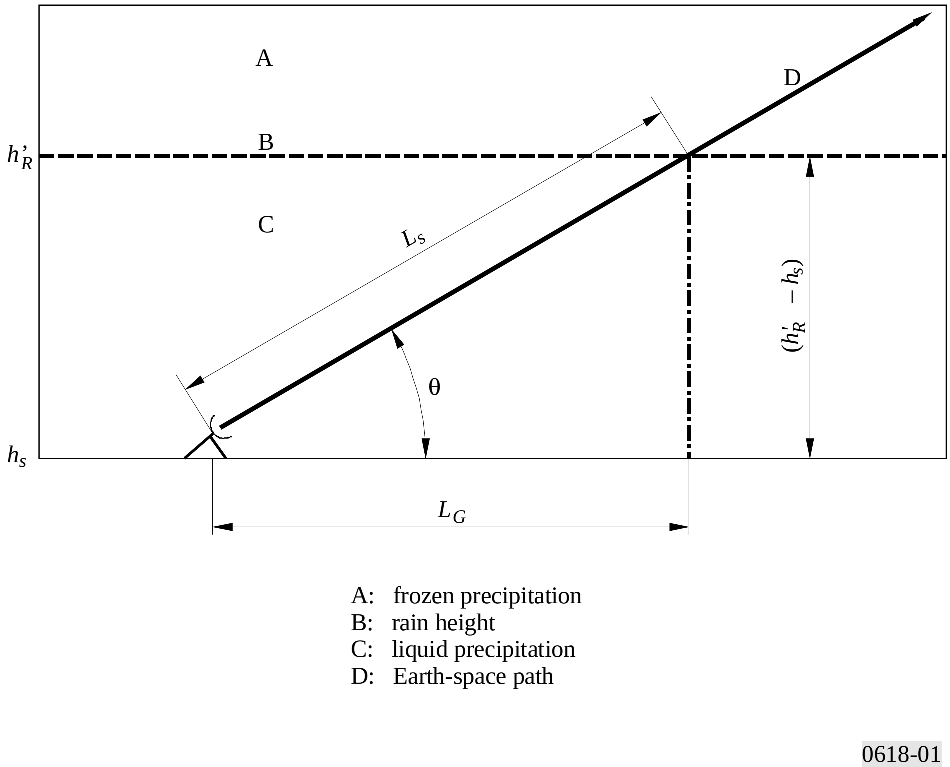

Step 1: Calculate the rain height, h'_R, which is equivalent to h_0 as given in Recommendation ITU-R P.839.

Step 2: For $\theta \geq 5°$ compute the slant-path length, L_s, below the rain height from:

$$L_s = \frac{(h'_R - h_s)}{\sin\theta} \qquad \text{km} \tag{4}$$

For $\theta < 5°$, the following formula is used:

$$L_s = \frac{2(h'_R - h_s)}{\left(\sin^2\theta + \frac{2(h'_R - h_s)}{R_e}\right)^{1/2} + \sin\theta} \qquad \text{km} \tag{5}$$

Step 3: Calculate the horizontal projection, L_G, of the slant-path length from:

$$L_G = L_s \cos\theta \qquad \text{km} \tag{6}$$

Step 4: Obtain the rainfall rate, $R_{0.01}$, exceeded for 0.01% of an average year (with an integration time of 1 min). If this long-term statistic cannot be obtained from local data sources, an estimate can be obtained from the maps of rainfall rate given in Recommendation ITU-R P.837.

Step 5: Obtain the specific attenuation, γ_R, using the frequency-dependent coefficients given in Recommendation ITU-R P.838 and the rainfall rate, $R_{0.01}$, determined from Step 4, by using:

$$\gamma_R = k\,(R_{0.01})^{\alpha} \qquad \text{dB/km} \tag{7}$$

Step 6: Calculate the horizontal reduction factor, $r_{0.01}$, for 0.01% of the time:

$$r_{0.01} = \frac{1}{1 + 0.78\sqrt{\dfrac{L_G\,\gamma_R}{f}} - 0.38\left(1 - e^{-2L_G}\right)} \tag{8}$$

Step 7: Calculate the vertical adjustment factor, $v_{0.01}$, for 0.01% of the time:

$$\zeta = \tan^{-1}\left(\frac{h'_R - h_s}{L_G\, r_{0.01}}\right) \qquad \text{degrees}$$

For $\zeta > \theta$,

$$L_R = \frac{L_G\, r_{0.01}}{\cos\theta} \qquad \text{km}$$

Else,

$$L_R = \frac{(h'_R - h_s)}{\sin\theta} \qquad \text{km}$$

If $|\,\varphi\,| < 36°$,

$$\chi = 36 - |\varphi| \qquad \text{degrees}$$

Else,

$$\chi = 0 \qquad \text{degrees}$$

$$\nu_{0.01} = \frac{1}{1 + \sqrt{\sin\theta}\left(31\left(1 - e^{-(\theta/(1+\chi))}\right)\dfrac{\sqrt{L_R\,\gamma_R}}{f^2} - 0.45\right)}$$

Step 8: The effective path length is:

$$L_E = L_R\,\nu_{0.01} \qquad \text{km} \tag{9}$$

Step 9: The predicted attenuation exceeded for 0.01% of an average year is obtained from:

$$A_{0.01} = \gamma_R\, L_E \qquad \text{dB} \tag{10}$$

Step 10: The estimated attenuation to be exceeded for other percentages of an average year, in the range 0.001% to 5%, is determined from the attenuation to be exceeded for 0.01% for an average year:

If $p \geq 1\%$ or $\lvert\varphi\rvert \geq 36°$:	$\beta = 0$
If $p < 1\%$ and $\lvert\varphi\rvert < 36°$ and $\theta \geq 25°$:	$\beta = -0.005(\lvert\varphi\rvert - 36)$
Otherwise:	$\beta = -0.005(\lvert\varphi\rvert - 36) + 1.8 - 4.25\sin\theta$

$$A_p = A_{0.01}\left(\frac{p}{0.01}\right)^{-(0.655 + 0.033\ln(p) - 0.045\ln(A_{0.01}) - \beta(1-p)\sin\theta)} \qquad \text{dB} \tag{11}$$

This method provides an estimate of the long-term statistics of attenuation due to rain. When comparing measured statistics with the prediction, allowance should be given for the rather large year-to-year variability in rainfall rate statistics (see Recommendation ITU-R P.678).

2.2.1.2 Long-term frequency and polarization scaling of rain attenuation statistics

The method of § 2.2.1.1 may be used to investigate the dependence of attenuation statistics on elevation angle, polarization and frequency, and is therefore a useful general tool for scaling of attenuation according to these parameters.

If reliable attenuation data measured at one frequency are available, the following empirical formula giving an attenuation ratio directly as a function of frequency and attenuation may be applied for frequency scaling on the same path in the frequency range 7 to 55 GHz:

$$A_2 = A_1 \left(\varphi_2 / \varphi_1 \right)^{1 - H(\varphi_1, \varphi_2, A_1)} \tag{12}$$

where:

$$\varphi(f) = \frac{f^2}{1 + 10^{-4} f^2} \tag{13a}$$

$$H(\varphi_1, \varphi_2, A_1) = 1.12 \times 10^{-3} (\varphi_2 / \varphi_1)^{0.5} (\varphi_1 A_1)^{0.55} \tag{13b}$$

A_1 and A_2 are the equiprobable values of the excess rain attenuation at frequencies f_1 and f_2 (GHz), respectively.

Frequency scaling from reliable attenuation data is preferred, when applicable, rather than the prediction methods starting from rain data.

When polarization scaling is required, it is more appropriate to use directly the parameters k and α as given in Recommendation ITU-R P.838. These parameters also provide a radiometeorological basis for frequency scaling.

2.2.2 Seasonal variations – worst month

System planning often requires the attenuation value exceeded for a time percentage, p_w, of the worst month. The following procedure is used to estimate the attenuation exceeded for a specified percentage of the worst month.

Step 1: Obtain the annual time percentage, p, corresponding to the desired worst-month time percentage, p_w, by using the equation specified in Recommendation ITU-R P.841 and by applying any adjustments to p as prescribed therein.

Step 2: For the path in question obtain the attenuation, A (dB), exceeded for the resulting annual time percentage, p, from the method of § 2.2.1.1, or from measured or frequency-scaled attenuation statistics. This value of A is the estimated attenuation for p_w per cent of the worst month.

Curves giving the variation of worst-month values from their mean are provided in Recommendation ITU-R P.678.

2.2.3 Variability in space and time of statistics

Precipitation attenuation distributions measured on the same path at the same frequency and polarization may show marked year-to-year variations. In the range 0.001% to 0.1% of the year, the attenuation values at a fixed probability level are observed to vary by more than 20% r.m.s. When the models for attenuation prediction or scaling in § 2.2.1 are used to scale observations at a location to estimate for another path at the same location, the variations increase to more than 25% r.m.s.

2.2.4 Site diversity

Intense rain cells that cause large attenuation values on an Earth-space link often have horizontal dimensions of no more than a few kilometres. Diversity systems able to re-route traffic to alternate earth stations, or with access to a satellite with extra on-board resources available for temporary allocation, can improve the system reliability considerably.

Two concepts exist for characterizing diversity performance: the diversity improvement factor is defined as the ratio of the single-site time percentage and the diversity time percentage, at the same attenuation level. Diversity gain is the difference (dB) between the single-site and diversity attenuation values for the same time percentage. Both parameters are important, depending on the system design approach, and prediction procedures for both are given below.

The procedures have been tested at frequencies between 10 and 30 GHz, which is the recommended frequency range of applicability. The diversity prediction procedures are only recommended for time percentages less than 0.1%. At time percentages above 0.1%, the rainfall rate is generally small and the corresponding site diversity improvement is not significant.

2.2.4.1 Diversity improvement factor

The diversity improvement factor, *I*, is given by:

$$I = \frac{p_1}{p_2} = \frac{1}{(1 + \beta^2)} \left(1 + \frac{100\,\beta^2}{p_1} \right) \approx 1 + \frac{100\,\beta^2}{p_1} \tag{14}$$

where p_1 and p_2 are the respective single-site and diversity time percentages, and β is a parameter depending on link characteristics. The approximation on the right-hand side of equation (14) is acceptable since β^2 is generally small.

From a large number of measurements carried out in the 10-20 GHz band, and mainly between 11 GHz and 13.6 GHz, it has been found that the value of β^2 depends basically on the distance, *d*, between the stations, and only slightly on the angle of elevation and the frequency. It is found that β^2 can be expressed by the following empirical relationship:

$$\beta^2 = 10^{-4}\, d^{1.33} \tag{15}$$

Figure 2 shows p_2 versus p_1 on the basis of equations (14) and (15).

FIGURE 2

Relationship between percentages of time with and without diversity for the same attenuation (Earth-satellite paths)

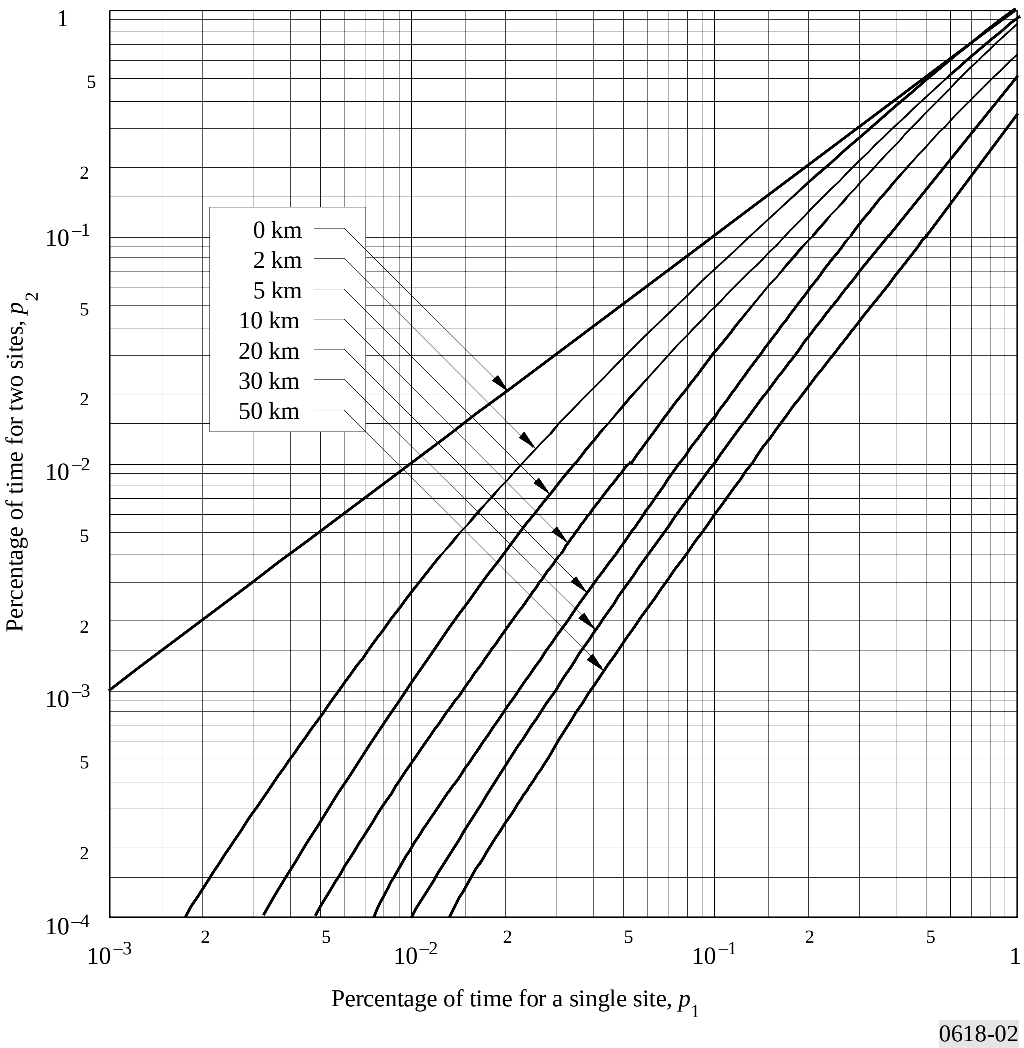

2.2.4.2 Diversity gain

The diversity gain, G (dB), between pairs of sites is calculated with the empirical expression given below. Parameters required for the calculation of diversity gain are:

- d: separation (km) between the two sites
- A: path rain attenuation (dB) for a single site
- f: frequency (GHz)
- θ: path elevation angle (degrees)
- ψ: angle (degrees) made by the azimuth of the propagation path with respect to the baseline between sites, chosen such that $\psi \leq 90°$.

Step 1: Calculate the gain contributed by the spatial separation from:

$$G_d = a\left(1 - e^{-bd}\right) \tag{16}$$

where:

$$a = 0.78\,A - 1.94\left(1 - e^{-0.11\,A}\right)$$

$$b = 0.59\left(1 - e^{-0.1\,A}\right)$$

Step 2: Calculate the frequency-dependent gain from:

$$G_f = e^{-0.025\,f} \tag{17}$$

Step 3: Calculate the gain term dependent on elevation angle from:

$$G_\theta = 1 + 0.006\,\theta \tag{18}$$

Step 4: Calculate the baseline-dependent term from the expression:

$$G_\psi = 1 + 0.002\,\psi \tag{19}$$

Step 5: Compute the net diversity gain as the product:

$$G = G_d \cdot G_f \cdot G_\theta \cdot G_\psi \qquad \text{dB} \tag{20}$$

When the above method was tested against the Radiocommunication Study Group 3 site diversity data bank, the arithmetic mean and standard deviation were found to be 0.14 dB and 0.96 dB, respectively, with an r.m.s. error of 0.97 dB.

2.2.5 Characteristics of precipitation events

2.2.5.1 Durations of individual fades

The durations of rain fades that exceed a specified attenuation level are approximately log-normally distributed. Median durations are of the order of several minutes. No significant dependence of these distributions on fade depth is evident in most measurements for fades of less than 20 dB, implying that the larger total time percentage of fades observed at lower fade levels or at higher frequencies is composed of a larger number of individual fades having more or less the same distribution of durations. Significant departures from log-normal seem to occur for fade durations of less than about half a minute. Fade durations at a specified fade level tend to increase with decreasing elevation angle.

For the planning of integrated services digital network (ISDN) connections via satellite, data are needed on the contribution of attenuation events shorter than 10 s to the total fading time. This information is especially relevant for the attenuation level corresponding to the outage threshold, where events longer than 10 s contribute to system unavailable time, while shorter events affect system performance during available time (see Recommendation ITU-R S.579). Existing data indicate that in the majority of cases, the exceedance time during available time is 2% to 10% of the net exceedance time. However, at low elevation angles where the short period signal fluctuations due to tropospheric scintillation become statistically significant, there are some cases for which the exceedance time during available time is far larger than in the case at higher elevation Earth-space paths.

2.2.5.2 Rates of change of attenuation (fading rate)

There is broad agreement that the distributions of positive and negative fade rates are log-normally distributed and very similar to each other. The dependence of fade rate on fade depth has not been established.

2.2.5.3 Correlation of instantaneous values of attenuation at different frequencies

Data on the instantaneous ratio of rain attenuation values at different frequencies are of interest for a variety of adaptive fade techniques. The frequency-scaling ratio has been found to be log-normally distributed, and is influenced by rain type and rain temperature. Data reveal that the short-term variations in the attenuation ratio can be significant, and are expected to increase with decreasing path elevation angle.

2.3 Clear-air effects

Other than atmospheric absorption, clear-air effects in the absence of precipitation are unlikely to produce serious fading in space telecommunication systems operating at frequencies below about 10 GHz and at elevation angles above 10°. At low elevation angles ($\leq 10°$) and at frequencies above about 10 GHz, however, tropospheric scintillations can on occasion cause serious degradations in performance. At very low elevation angles ($\leq 4°$ on inland paths, and $\leq 5°$ on overwater or coastal paths), fading due to multipath propagation effects can be particularly severe. At some locations, ionospheric scintillation may be important at frequencies below about 6 GHz (see Recommendation ITU-R P.531).

2.3.1 Decrease in antenna gain due to wave-front incoherence

Incoherence of the wave-front of a wave incident on a receiving antenna is caused by small-scale irregularities in the refractive index structure of the atmosphere. Apart from the rapid signal fluctuations discussed in § 2.4, they cause an antenna-to-medium coupling loss that can be described as a decrease of the antenna gain.

This effect increases both with increasing frequency and decreasing elevation angle, and is a function of antenna diameter. Although not explicitly accounted for in the refraction models presented below, this effect is negligible in comparison.

2.3.2 Beam spreading loss

The regular decrease of refractive index with height causes ray-bending and hence a defocusing effect at low angles of elevation (Recommendation ITU-R P.834). The magnitude of the defocusing loss of the antenna beam is independent of frequency, over the range of 1-100 GHz.

The loss A_{bs} due to beam spreading in regular refractive conditions can be ignored at elevation angles above about 3° at latitudes less than 53° and above about 6° at higher latitudes.

At all latitudes, the beam spreading loss in the average year at elevation angles less than 5° is estimated from:

$$A_{bs} = 2.27 - 1.16 \log (1 + \theta_0) \qquad \text{dB} \qquad \text{for } A_{bs} > 0 \tag{21}$$

where θ_0 is the apparent elevation angle (mrad) taking into account the effects of refraction. The beam spreading loss in the average worst month at latitudes less than 53° is also estimated from equation (21).

At latitudes greater than 60°, the beam spreading loss at elevation angles less than 6° in the average worst month is estimated from:

$$A_{bs} = 13 - 6.4 \log (1 + \theta_0) \qquad \text{dB} \qquad \text{for } A_{bs} > 0 \tag{22}$$

At latitudes ψ between 53° and 60°, the median beam spreading loss can be estimated by a linear interpolation between the values obtained from equation (21) (designated A_{bs} (< 53°)) and equation (22) (designated A_{bs} (> 60°)) as follows:

$$A_{bs} = A_{bs}\left(> 60°\right) - \frac{60}{7}\,\Delta A_{bs} + \frac{1}{7}\,\Delta A_{bs}\,\psi \qquad \text{dB} \tag{23}$$

where $\Delta A_{bs} = A_{bs}\,(> 60°) - A_{bs}\,(< 53°)$.

2.4 Scintillation and multipath fading

The magnitude of tropospheric scintillations depends on the magnitude and structure of the refractive index variations, increasing with frequency and with the path length through the medium, and decreasing as the antenna beamwidth decreases because of aperture averaging. Monthly-averaged r.m.s. fluctuations are well-correlated with the wet term of the radio refractivity, N_{wet}, which depends on the water vapour content of the atmosphere. N_{wet} may be estimated for periods of a month or longer from meteorological data obtained at the surface.

At very small percentages of time, or conversely large fade depths (greater than about 10 dB), the fading at very low elevation angles ($\leq 4°$, and $\leq 5°$ for links over water or in coastal areas) is observed to be more severe than that predicted due to scintillation. The fading is also observed to have a character similar to multipath fading on terrestrial links. Like the distribution on terrestrial links, the distribution for very-low-angle satellite links also appears correlated with refractivity gradient statistics. The overall fading distribution shows a gradual transition from a scintillation distribution at large exceedance percentages to a multipath fading distribution (with a slope of 10 dB/decade) at small percentages. The methods in § 2.4.2 and 2.4.3, for the deep fading and shallow fading portions of the overall distribution, respectively, use the refractivity gradient statistic p_L for describing climatic variations in the distribution.

For overwater and coastal paths with elevation angles in the 4° to 5° range, the methods of § 2.4.2 and 2.4.3 should be applied as well as the method of § 2.4.1, and the one giving the largest fade depths then employed in estimates of path fading statistics.

The net fade distribution due to tropospheric refractive effects, A_{ref} (p), is the combination of the beam spreading, scintillation, and multipath-fading effects described above. Tropospheric and ionospheric scintillation distributions may be combined by summing the respective time percentages that specified fade levels are exceeded.

2.4.1 Calculation of monthly and long-term statistics of amplitude scintillations at elevation angles greater than 4°

A general technique for predicting the cumulative distribution of tropospheric scintillation at elevation angles greater than 4° is given below. It is based on monthly or longer averages of temperature t (°C) and relative humidity H, and reflects the specific climatic conditions of the site. As the averages of t and H vary with season, distributions of scintillation fade depth exhibit seasonal variations, which may also be predicted by using seasonal averages of t and H in the method. Values of t and H may be obtained from weather information for the site(s) in question.

The procedure has been tested at frequencies between 7 and 14 GHz, but is recommended for applications up to at least 20 GHz.

Parameters required for the method include:

t: average surface ambient temperature (°C) at the site for a period of one month or longer

H: average surface relative humidity (%) at the site for a period of one month or longer

f: frequency (GHz), where 4 GHz $\leq f \leq$ 20 GHz

θ: path elevation angle, where $\theta \geq 4°$

D: physical diameter (m) of the earth-station antenna

η: antenna efficiency; if unknown, $\eta = 0.5$ is a conservative estimate.

Step 1: For the value of t, calculate the saturation water vapour pressure, e_s, (hPa), as specified in Recommendation ITU-R P.453.

Step 2: Compute the wet term of the radio refractivity, N_{wet}, corresponding to e_s, t and H as given in Recommendation ITU-R P.453.

Step 3: Calculate the standard deviation of the signal amplitude, σ_{ref}, used as reference:

$$\sigma_{ref} = 3.6 \times 10^{-3} + 10^{-4} \times N_{wet} \qquad \text{dB} \tag{24}$$

Step 4: Calculate the effective path length L according to:

$$L = \frac{2h_L}{\sqrt{\sin^2 \theta + 2.35 \times 10^{-4}} + \sin \theta} \qquad \text{m} \tag{25}$$

where h_L is the height of the turbulent layer; the value to be used is $h_L = 1\,000$ m.

Step 5: Estimate the effective antenna diameter, D_{eff}, from the geometrical diameter, D, and the antenna efficiency η:

$$D_{eff} = \sqrt{\eta}\, D \qquad \text{m} \tag{26}$$

Step 6: Calculate the antenna averaging factor from:

$$g(x) = \sqrt{3.86 \ (x^2 + 1)^{11/12} \cdot \sin\left[\frac{11}{6} \arctan \frac{1}{x}\right] - 7.08\, x^{5/6}} \tag{27}$$

with:

$$x = 1.22\, D_{eff}^2 (f/L)$$

where f is the carrier frequency (GHz).

Step 7: Calculate the standard deviation of the signal for the considered period and propagation path:

$$\sigma = \sigma_{ref} \ f^{7/12} \frac{g(x)}{(\sin \theta)^{1.2}} \tag{28}$$

Step 8: Calculate the time percentage factor, $a(p)$, for the time percentage, p, of concern in the range $0.01 < p \leq 50$:

$$a(p) = -0.061\,(\log_{10} p)^3 + 0.072\,(\log_{10} p)^2 - 1.71 \log_{10} p + 3.0 \tag{29}$$

Step 9: Calculate the scintillation fade depth for the time percentage p by:

$$A_s(p) = a(p) \cdot \sigma \qquad \text{dB} \tag{30}$$

2.4.2 Calculation of the deep fading part of the scintillation/multipath fading distribution of elevation angles less than 5°

This method estimates the large fade depth range (typically fades larger than about 25 dB) of the combined beam spreading, scintillation and multipath fading distribution of A_{ref} in the average worst month and average year (predictions for the average year being derived from those for the average worst month). The method also serves as a basis for the interpolation procedure given in § 2.4.3 for predicting the shallow fading range of the distribution. The step-by-step procedure is as follows:

Step 1: Obtain the apparent boresight elevation angle θ_0 (mrad) (taking account of the effects of refraction) for the path location in question (see Recommendation ITU-R P.834).

Step 2: For the path location in question, obtain the geoclimatic factor, K_w, applicable for the average worst month from:

$$K_w = 10^{0.1\left(C_0 + C_{Lat}\right)} \ p_L^{\ 1.5} \tag{31}$$

The variable p_L is the percentage of time that the refractivity gradient in the lowest 100 m of the atmosphere is less than –100 N units/km in that month having the highest value of p_L from the four seasonally representative months of February, May, August and November for which maps are given in Figs. 7 to 10 of Recommendation ITU-R P.453.

As an exception, only the maps for May and August should be used for latitudes greater than 60° N or 60° S.

The values of the coefficient C_0 in equation (31) and the conditions for their applicability are summarized in Table 3. The coefficient C_{Lat} of latitude ψ (in °N or °S) is given by:

$$C_{Lat} = 0 \qquad \text{for} \qquad 53° \text{ S} \geq \psi \leq 53° \text{ N} \tag{32}$$

$$C_{Lat} = -53 + \psi \qquad \text{for} \qquad 53° \text{ N or S} < \psi < 60° \text{ N or S} \tag{33}$$

$$C_{Lat} = 7 \qquad \text{for} \qquad \psi \geq 60° \text{ N or S} \tag{34}$$

TABLE 3

Values of the coefficient C_0 in equation (31) for various types of propagation path

Type of path	C_0
Propagation paths[(1)] entirely over land for which the earth-station antenna is less than 700 m above mean sea level[(2)]	76
Propagation paths for which the earth-station antenna is higher than 700 m above mean sea level	70
Propagation paths entirely or partially over water or coastal areas beside such bodies of water (see[(1)] for definition of propagation path, coastal areas, and definition of *r*)	$76 + 6r$

[(1)] The propagation path is the lowest portion of the Earth-space path over which the relevant tropospheric fading mechanisms are believed to occur. The approximate length of the propagation path is given by:

$$d_{eff} = 14\,000(1 + \theta_0)^{-1.3} \qquad \text{km} \qquad d_{eff} \leq 300 \text{ km} \tag{35}$$

where θ_0 is the boresight elevation angle (mrad).

The propagation path is considered to be crossing a coastal area if a section of the path profile (i.e. the profile of terrain altitudes over a distance along the path equal to that given by equation (35)) is less than 100 m above mean sea level (or the mean level of large inland bodies of water) or within 50 km of the coastline, and if there is no height of land above 100 m altitude between the propagation path and the coast.

The variable *r* in the expression for C_0 is the fraction of the propagation path that crosses a body of water or adjacent coastal areas.

[(2)] Propagation paths passing over a small lake or river are classed as being entirely over land. Although such bodies of water could be included in the calculation of *r*, this yields negligible increases in the value of the coefficient C_0 from the overland non-coastal values.

Step 3: Calculate the percentage of time that fade depth A_{ref} (dB) is exceeded in the average worst month from the power-law expression:

$$p = K_w \, f^{0.9}(1 + \theta_0)^{-5.5} \times 10^{-A_{ref}/10} \qquad \% \tag{36}$$

Alternatively, calculate the fade depth, A_{ref}, exceeded for p% of the time at frequency, f, in the average worst month from:

$$A_{ref} = G_w + 92 + 9 \log f - 55 \log (1 + \theta_0) - 10 \log p \qquad \text{dB} \tag{37}$$

where G_w is the logarithmic geoclimatic factor for the average worst month given by:

$$G_w = 10 \log K_w - 92 \qquad \text{dB} \tag{38}$$

Step 4: Calculate the percentage of time that fade depth A_{ref} (dB) is exceeded in the average year from equation (36), with K_w replaced by K_a, where:

$$K_a = K_w \times 10^{-0.1\,\Delta G} \tag{39}$$

with:

$$\Delta G = -1.8 - 5.6 \log\left(1.1 \pm |\cos 2\psi|^{0.7}\right) + 4.5 \log (1 + \theta_0) \qquad \text{dB} \tag{40}$$

The positive sign in equation (40) is employed for latitude $\psi \le 45$ (°N or °S) and the negative sign for $\psi > 45°$. Alternatively, calculate the fade depth A_{ref} exceeded for p% of the time at frequency f in the average year from equation (37), with G_w replaced by $G_a = G_w - \Delta G$.

Equations (36) and (37) are valid for A_{ref} greater than about 25 dB. They were developed from data in the frequency range 6-38 GHz and elevation angles in the range of 1° to 4°. They are expected to be valid at least in the frequency range 1-45 GHz and elevation angles in the range of 0.5° to 5°.

2.4.3 Calculation of the shallow fading part of the scintillation/multipath fading distribution at elevation angles less than 5°

Step 1: Estimate the fade depth A_{ref} (63%) exceeded for 63% of the average worst month or average year (denoted A_{63}) as desired, as follows: at latitudes greater than 60° in the average worst month, use:

$$A_{63} = 9.4 - 4.5 \log(1 + \theta_0) \qquad \text{dB} \qquad \text{for } A_{bs} > 0 \tag{41}$$

where θ_0 is again the apparent elevation angle (mrad). At latitudes less than 53°, use the expression in equation (21). At latitudes between 53° and 60°, carry out a linear interpolation as in equation (23). For average-year calculations, use equation (21) for all latitudes.

Step 2: For average-worst-month predictions, calculate the percentage of time p_t that fade depth of $A_t = 25$ dB is exceeded in the multipath tail of the distribution using equation (36). For average year predictions, replace K_w in equation (36) by K_a in equation (39) for this calculation.

Step 3: Calculate the new percentage of time p from:

$$p = 10^{-0.1\, A_{63} + \log p_t} \qquad \% \tag{42}$$

Step 4: Calculate the value of the parameter q' corresponding to the fade depth A_t and percentage of time p from:

$$q' = -\frac{20}{A_t} \log_{10} \left[-\ln \left(\frac{100 - p}{100} \right) \right] \tag{43}$$

Step 5: Calculate the values of the shape factor q_t from:

$$q_t = (q' - 2) \Big/ \left[\left(1 + 0.3 \times 10^{-A_t/20}\right) \times 10^{-0.016\, A_t} \right] - s_0 \left(10^{-A_t/20} + A_t/800\right) \tag{44}$$

where:

$$s_0 = -1.6 - 3.2 \log f + 4.2 \log(1 + \theta_0) \tag{45}$$

with:

f: frequency (GHz)

θ_0: apparent elevation angle (mrad).

Step 6: If $q_t < 0$, repeat Steps 2 to 5 for $A_t = 35$ dB to obtain the definitive value of q_t.

Step 7: For $A_{63} < A_{ref}(p) < 25 + A_{63}$ dB or $A_{63} < A_{ref}(p) < 35 + A_{63}$ dB, depending on the value required for A_t, calculate the percentage of time p that A_{ref} is exceeded using the following:

$$p = 100 \left[1 - \exp\left(-10^{-q(A_{ref} - A_{63})/20} \right) \right] \qquad \% \tag{46}$$

where q is also a function of A_{ref} and is given by:

$$q = 2 + 10^{-0.016(A_{ref} - A_{bs})} \left[1 + 0.3 \times 10^{-(A_{ref} - A_{bs})/20} \right] \cdot \left[q_t + s_0 \left(10^{-(A_{ref} - A_{63})/20} + (A_{ref} - A_{63})/800 \right) \right] \tag{47}$$

Here the value of the parameter q_t is that obtained in Step 5 or 6, as appropriate.

For $A_{ref} \geq 25 + A_{63}$ dB or $A_{ref} \geq 35 + A_{63}$ dB, depending on the value required for A_t, calculate the percentage of time p that A_{ref} is exceeded from equation (36).

Step 8: For $A_{ref}(p) < A_{ref}(63\%)$, and for the enhancement range of the distribution, the enhancement relative to A_{ref} (63%) is expressed as:

$$E_{ref}(p_e) = A_{ref}(63\%) - A_{ref}(p) \qquad \text{dB} \tag{48}$$

This enhancement, exceeded for percentages p_e of the time (not exceeded for $p = 100 - p_e\%$ of the time), can be approximated using the method of § 2.3.3 of Recommendation ITU-R P.530:

– In applying this method for the average worst month, the calculation of the fade depth $A_{0.01}$ exceeded for 0.01% of the average worst month should be obtained using equation (37) in place of the equations for terrestrial links.

– In applying the method for the average year, equation (37) should be employed with G_w replaced by G_a as obtained in Step 4 following equation (37).

It should be noted that this method can underpredict the relative enhancement by up to 78% at $p_e = 10\%$ and 47% at $p_e = 1\%$. Reasonable accuracy is achieved for the small percentages $p_e < 0.1\%$ of greatest interest.

The method in Steps 1 to 7 is valid for values of q_t greater than –1.5, which covers virtually all the combined ranges of K, f and θ_0 most likely to arise under operational circumstances. For values of q_t less than –1.5, the method is not recommended. The method implicitly includes the beam-spreading loss discussed in § 2.3.2.

2.5 Estimation of total attenuation due to multiple sources of simultaneously occurring atmospheric attenuation

For systems operating at frequencies above about 18 GHz, and especially those operating with low elevation angles and/or margins, the effect of multiple sources of simultaneously occurring atmospheric attenuation must be considered.

Total attenuation (dB) represents the combined effect of rain, gas, clouds and scintillation and requires one or more of the following input parameters:

$A_R(p)$: attenuation due to rain for a fixed probability (dB), as estimated by A_p in equation (11)

$A_C(p)$: attenuation due to clouds for a fixed probability (dB), as estimated by Recommendation ITU-R P.840

A_G: mean gaseous attenuation due to water vapour and oxygen (dB), as estimated by Recommendation ITU-R P.676.

$A_S(p)$: attenuation due to tropospheric scintillation for a fixed probability (dB), as estimated by equation (30)

where p is the probability of the attenuation being exceeded in the range 50% to 0.001%.

A general method for calculating total attenuation for a given probability, $A_T(p)$, is given by:

$$A_T(p) = A_G + \sqrt{\left(A_R(p) + A_C(p)\right)^2 + A_S^2(p)} \tag{49}$$

However, for $p < 1.0\%$, $A_C(p) = 0$ because cloud attenuation is already included in the rain attenuation prediction. The use of this method may be simplified with minimal impact on accuracy by making certain assumptions when considering operation in different weather conditions as summarized in Table 4. However, the application of these assumptions is climate dependent, and local weather measurements should be referenced.

TABLE 4

Simplifying assumptions to equation (49) for various weather conditions

Condition	Simplifying assumption
Rain dominated	In most parts of the world, except dry climates rain will dominate the total attenuation when $1.0\% > p > 0.001\%$. In this case the other effects may be neglected and the total attenuation given in equation (49) reduces to: $$A_T(p) = A_R(p) \quad (50)$$
Multiple effects	In most parts of the world, except dry climates, all effects may contribute a measurable level of propagation impairment when $5.0\% \geq p \geq 1.0\%$. However, for elevation angles above about 10° the effect of scintillation may become negligible. In this case, equation (49) reduces to: $$A_T(p) = A_G + A_R(p) + A_C(p) \quad (51)$$
Non-raining	In most parts of the world, except very wet climates, the non-rainy condition is present when $p > 5\%$. During clear air conditions, rain attenuation is, by definition, 0 dB. In this case, equation (49) reduces to: $$A_T(p) = A_G + \sqrt{A_C^2(p) + A_S^2(p)} \quad (52)$$ When operating at elevation angles greater than about 10°, scintillation may become negligible during clear air conditions and equation (52) will further reduce to: $$A_T(p) = A_G + A_C(p) \quad (53)$$

When the complete prediction method above was tested using the procedure set out in Annex 1 to Recommendation ITU-R P.311, the results were found to be in good agreement with available measurement data for all latitudes and in the probability range 0.001% to 1%, with an overall r.m.s. error of about 35%, when used with the contour rain maps in Recommendation ITU-R P.837. When tested against multi-year Earth-space data, the overall r.m.s. error was found to be about 25%. Due to the dominance of different effects at different probabilities as well as the inconsistent availability of test data at different probability levels, some variation of r.m.s. error occurs across the distribution of probabilities.

2.6 Attenuation by sand and dust storms

Very little is known about the effects of sand and dust storms on radio signals on slant-paths. Available data indicate that at frequencies below 30 GHz, high particle concentrations and/or high moisture contents are required to produce significant propagation effects.

3 Noise temperature

As attenuation increases, so does emission noise. For earth stations with low-noise front-ends, this increase of noise temperature may have a greater impact on the resulting signal-to-noise ratio than the attenuation itself.

The atmospheric contribution to antenna noise in a ground station may be estimated with the equation:

$$T_s = T_m \left(1 - 10^{-A/10} \right) \quad (54)$$

where:

T_s: sky-noise temperature (K) as seen by the antenna

A: path attenuation (dB)

T_m: effective temperature (K) of the medium.

The effective temperature is dependent on the contribution of scattering to attenuation and on the physical extent of clouds and rain cells on the vertical variation of the physical temperature of the scatterers and, to a lesser extent, on the antenna beamwidth. By comparing radiometric observations and simultaneous beacon attenuation measurements, the effective temperature of the medium has been determined to lie in the range 260-280 K for rain and clouds along the path at frequencies between 10 and 30 GHz.

When the attenuation is known, the following effective temperatures of the mediums may be used to obtain an upper limit to sky-noise temperature at frequencies below 60 GHz:

$$T_m = 280 \text{ K for clouds}$$

$$T_m = 260 \text{ K for rain}$$

The noise environments of stations on the surface of the Earth and in space are treated in detail in Recommendation ITU-R P.372.

For satellite telecommunication systems using the geostationary orbit, earth stations will find that the Sun and, to a lesser extent, the Moon, are significant noise sources at all frequencies and that the galactic background is a possibly significant consideration at frequencies below about 2 GHz (see Recommendation ITU-R P.372). In addition, contributions to the sky background noise temperature may be given by Cygnus A and X, Cassiopeia A, Taurus and The Crab nebula.

To determine the system noise temperature of earth stations from the brightness temperatures discussed above, the equations of Recommendation ITU-R P.372 may be used.

4 Cross-polarization effects

Frequency re-use by means of orthogonal polarizations is often used to increase the capacity of space telecommunication systems. This technique is restricted, however, by depolarization on atmospheric propagation paths. Various depolarization mechanisms, especially hydrometeor effects, are important in the troposphere.

Faraday rotation of the plane of polarization by the ionosphere is discussed in Recommendation ITU-R P.531. As much as 1° of rotation may be encountered at 10 GHz, and greater rotations at lower frequencies. As seen from the earth station, the planes of polarization rotate in the same direction on the up- and down-links. It is therefore not possible to compensate for Faraday rotation by rotating the feed system of the antenna, if the same antenna is used both for transmitting and receiving.

4.1 Calculation of long-term statistics of hydrometeor-induced cross-polarization

To calculate long-term statistics of depolarization from rain attenuation statistics the following parameters are needed:

- A_p: rain attenuation (dB) exceeded for the required percentage of time, *p*, for the path in question, commonly called co-polar attenuation (CPA)
- τ: tilt angle of the linearly polarized electric field vector with respect to the horizontal (for circular polarization use $\tau = 45°$)
- f: frequency (GHz)
- θ: path elevation angle (degrees).

The method described below to calculate cross-polarization discrimination (XPD) statistics from rain attenuation statistics for the same path is valid for $8 \le f \le 35$ GHz and $\theta \le 60°$. The procedure for scaling to frequencies down to 4 GHz is given in § 4.3 (and see Step 8 below).

Step 1: Calculate the frequency-dependent term:

$$C_f = 30 \log f \qquad \text{for } 8 \le f \le 35 \text{ GHz} \tag{55}$$

Step 2: Calculate the rain attenuation dependent term:

$$C_A = V(f) \log A_p \tag{56}$$

where:

$$V(f) = 12.8 f^{0.19} \qquad \text{for } 8 \le f \le 20 \text{ GHz}$$

$$V(f) = 22.6 \qquad \text{for } 20 < f \le 35 \text{ GHz}$$

Step 3: Calculate the polarization improvement factor:

$$C_\tau = -10 \log \left[1 - 0.484 \left(1 + \cos 4\tau\right)\right] \tag{57}$$

The improvement factor $C_\tau = 0$ for $\tau = 45°$ and reaches a maximum value of 15 dB for $\tau = 0°$ or $90°$.

Step 4: Calculate the elevation angle-dependent term:

$$C_\theta = -40 \log (\cos \theta) \qquad \text{for } \theta \le 60° \tag{58}$$

Step 5: Calculate the canting angle dependent term:

$$C_\sigma = 0.0052\, \sigma^2 \tag{59}$$

σ is the effective standard deviation of the raindrop canting angle distribution, expressed in degrees; σ takes the value 0°, 5°, 10° and 15° for 1%, 0.1%, 0.01% and 0.001% of the time, respectively.

Step 6: Calculate rain XPD not exceeded for p% of the time:

$$XPD_{rain} = C_f - C_A + C_\tau + C_\theta + C_\sigma \qquad \text{dB} \tag{60}$$

Step 7: Calculate the ice crystal dependent term:

$$C_{ice} = XPD_{rain} \times (0.3 + 0.1 \log p)/2 \qquad \text{dB} \tag{61}$$

Step 8: Calculate the XPD not exceeded for p% of the time, including the effects of ice:

$$XPD_p = XPD_{rain} - C_{ice} \qquad \text{dB} \tag{62}$$

In this prediction method in the frequency band 4 to 6 GHz where path attenuation is low, A_p statistics are not very useful for predicting XPD statistics. For frequencies below 8 GHz, the frequency-scaling formula of § 4.3 can be used to scale cross-polarization statistics calculated for 8 GHz down to the 6 to 4 GHz band.

4.2 Joint statistics of XPD and attenuation

The conditional probability distribution of XPD for a given value of attenuation, A_p, can be modelled by assuming that the cross-polar to co-polar voltage ratio, $r = 10^{-XPD/20}$, is normally distributed. Parameters of the distribution are the mean value, r_m, which is very close to $10^{-XPD_{rain}/20}$, with XPD_{rain} given by equation (60), and the standard deviation, σ_r, which assumes the almost-constant value of 0.038 for 3 dB $\le A_p \le$ 8 dB.

4.3 Long-term frequency and polarization scaling of statistics of hydrometeor-induced cross-polarization

Long-term XPD statistics obtained at one frequency and polarization tilt angle can be scaled to another frequency and polarization tilt angle using the semi-empirical formula:

$$XPD_2 = XPD_1 - 20 \log \left[\frac{f_2 \sqrt{1 - 0.484\ (1 + \cos 4\tau_2)}}{f_1 \sqrt{1 - 0.484\ (1 + \cos 4\tau_1)}} \right] \qquad \text{for } 4 \le f_1, f_2 \le 30 \text{ GHz} \tag{63}$$

where XPD_1 and XPD_2 are the XPD values not exceeded for the same percentage of time at frequencies f_1 and f_2 and polarization tilt angles, τ_1 and τ_2, respectively.

Equation (63) is based on the same theoretical formulation as the prediction method of § 4.1, and can be used to scale XPD data that include the effects of both rain and ice depolarization, since it has been observed that both phenomena have approximately the same frequency dependence at frequencies less than about 30 GHz.

4.4 Data relevant to cross-polarization cancellation

Experiments have shown that a strong correlation exists between rain depolarization at 6 and 4 GHz on Earth-space paths, both on the long term and on an event basis, and up-link depolarization compensation utilizing concurrent down-link depolarization measurements appears feasible. Only differential phase effects were apparent, even for severe rain events, and single-parameter compensation (i.e. for differential phase) appears sufficient at 6 and 4 GHz.

Measurements at 6 and 4 GHz have also shown that 99% of the XPD variations are slower than ± 4 dB/s, or equivalently, less than ± 1.5°/s in the mean path differential phase shift. Therefore, the time constant of a depolarization compensation system at these frequencies need only be about 1 s.

5 Propagation delays

Radiometeorologically-based methods for estimating the average propagation delay or range error, and the corresponding variations, for Earth-space paths through the troposphere are available in Recommendation ITU-R P.834. The delay variance is required for satellite ranging and synchronization in digital satellite communication systems. At frequencies above 10 GHz, the ionospheric time delay (see Recommendation ITU-R P.531) is generally smaller than that for the troposphere, but may have to be considered in special cases.

Range determination to centimetre accuracy requires careful consideration of the various contributions to excess range delay. The water vapour component amounts to 10 cm for a zenith path and a reference atmosphere with surface water vapour concentration of 7.5 g/m^3 and 2 km scale height (see Recommendation ITU-R P.676). This contribution is the largest source of uncertainty, even though the dry atmosphere adds 2.3 m of the zenithal excess range delay.

For current satellite telecommunication applications, additional propagation delays contributed by precipitation are sufficiently small to be ignored.

6 Bandwidth limitations

In the vicinity of the absorption lines of atmospheric gases, anomalous dispersion produces small changes in the refractive index. However, these refractive index changes are small in the bands allocated to Earth-space communications, and will not restrict the bandwidth of systems.

Multiple scattering in rain can limit the bandwidth of incoherent transmission systems due to variation in time delays of the multiple-scattered signals; however, the attenuation itself under such circumstances will present a far more serious problem. A study of the problem of bandwidth limitations imposed by the frequency dependence of attenuation and phase shift due to rain on coherent transmission systems showed that such bandwidth limitations are in excess of 3.5 GHz for all situations likely to be encountered. These are greater than any bandwidth allocated for Earth-space communications below 40 GHz, and the rain attenuation will therefore be far more important than its frequency dependence.

7 Angle of arrival

Elevation-angle errors due to refraction are discussed in Recommendation ITU-R P.834. The total angular refraction (the increase in apparent elevation) is about 0.65°, 0.35° and 0.25°, for elevation angles of 1°, 3° and 5°, respectively, for a tropical maritime atmosphere. For a polar continental climate the corresponding values are 0.44°, 0.25° and 0.17°. Other climates will have values between these two extremes. The day-to-day variation in apparent elevation is of the order of 0.1° (r.m.s.) at 1° elevation, but the variation decreases rapidly with increasing elevation angle.

Short-term angle-of-arrival fluctuations are discussed in Recommendation ITU-R P.834. Short-term variations, due to changes in the refractivity-height variation, may be of the order of 0.02° (r.m.s.) at 1° elevation, again decreasing rapidly with increasing elevation angle. In practice, it is difficult to distinguish between the effect of the short-term changes in the refractivity-height distribution and the effect of random irregularities superimposed on that distribution. A statistical analysis of the short-term angle-of-arrival fluctuation at 19.5 GHz and at an elevation angle of 48° suggests that both in elevation and azimuth directions, standard deviations of angle-of-arrival fluctuations are about 0.002° at the cumulative time percentage of 1%. The seasonal variation of angle-of-arrival fluctuations suggests that the fluctuations increase in summer and decrease in winter. The diurnal variation suggests that they increase in the daytime and decrease both in the early morning and the evening.

8 Calculation of long-term statistics for non-GSO paths

The prediction methods described above were derived for applications where the elevation angle remains constant. For non-GSO systems, where the elevation angle is varying, the link availability for a single satellite can be calculated in the following way:

a) calculate the minimum and maximum elevation angles at which the system will be expected to operate;

b) divide the operational range of angles into small increments (e.g. 5° wide);

c) calculate the percentage of time that the satellite is visible as a function of elevation angle in each increment;

d) for a given propagation impairment level, find the time percentage that the level is exceeded for each elevation angle increment;

e) for each elevation angle increment, multiply the results of c) and d) and divide by 100, giving the time percentage that the impairment level is exceeded at this elevation angle;

f) sum the time percentage values obtained in e) to arrive at the total system time percentage that the impairment level is exceeded.

In the case of multi-visibility satellite constellations employing satellite path diversity (i.e. switching to the least impaired path), an approximate calculation can be made assuming that the spacecraft with the highest elevation angle is being used.